

Article

Rheology, Hydration, and Microstructure of Portland Cement Pastes Produced with Ground Açai Fibers

Afonso Azevedo ¹, Paulo de Matos ^{2,3} , Markssuel Marvila ⁴ , Rafael Sakata ², Laura Silvestro ², Philippe Gleize ²  and Jorge de Brito ^{5,*} 

¹ LECIV—Civil Engineering Laboratory, UENF—State University of the Northern Rio de Janeiro, Av. Alberto Lamego, 2000, Campos dos Goytacazes 28013-602, Brazil; afonso@uenf.br

² Department of Civil Engineering, UFSC—Federal University of Santa Catarina, Rua João Pio Duarte Silva, 205, Florianópolis 88040-900, Brazil; paulo.matos@ufsm.br (P.d.M.); rafael.sakata@posgrad.ufsc.br (R.S.); laura.silvestro@posgrad.ufsc.br (L.S.); p.gleize@ufsc.br (P.G.)

³ Coordenadoria Acadêmica, UFSM—Federal University of Santa Maria, Rodovia Taufik Germano, 3013, Cachoeira do Sul 96503-205, Brazil

⁴ LAMAV—Advanced Materials Laboratory, UENF—State University of the Northern Rio de Janeiro, Av. Alberto Lamego, 2000, Campos dos Goytacazes 28013-602, Brazil; m.marvila@ucam-campos.br

⁵ CERIS, Instituto Superior Técnico, Universidade de Lisboa, Av. Rovisco Pais, 1049-01 Lisboa, Portugal

* Correspondence: jb@civil.ist.utl.pt

Abstract: Açai (*Euterpe oleracea*) is a Brazilian typical fruit that is enveloped by natural fibers. This work investigated the effect of incorporating ground açai fibers (in natura and chemically treated with NaOH and HCl) in 5–10 wt.% replacement of Portland cement on the rheology, hydration, and microstructure of pastes. Rotational rheometry, isothermal calorimetry, X-Ray Diffraction (XRD), and Scanning Electron Microscopy (SEM) were performed to evaluate the cement pastes, in addition to SEM-EDS, FTIR, zeta potential, and XRD for fiber characterization. The results showed that the chemical treatment reduced the cellulose and lignin contents in açai fibers while increasing its surface roughness. The addition of 5% of either fiber slightly increased the yield stress and viscosity of paste, while 10% addition drastically increased these properties, reaching yield stress and viscosity values respectively 40 and 8 times higher than those of plain paste. The incorporation of 5% in natura fibers delayed the cement hydration by about 2.5 days while 10% in natura fibers delayed it by over 160 h. The chemical treatment significantly reduced this retarding effect, leading to a 3 h delay when 5% treated fibers were incorporated. Overall, the combined NaOH/HCl treatment was effective for açai fibers functionalization and these fibers can be used in cementitious composites.

Keywords: açai fiber; cement pastes; rheology; hydration; microstructure



Citation: Azevedo, A.; de Matos, P.; Marvila, M.; Sakata, R.; Silvestro, L.; Gleize, P.; Brito, J.d. Rheology, Hydration, and Microstructure of Portland Cement Pastes Produced with Ground Açai Fibers. *Appl. Sci.* **2021**, *11*, 3036. <https://doi.org/10.3390/app11073036>

Academic Editor: Panagiotis G. Asteris

Received: 26 February 2021

Accepted: 24 March 2021

Published: 29 March 2021

Publisher's Note: MDPI stays neutral with regard to jurisdictional claims in published maps and institutional affiliations.



Copyright: © 2021 by the authors. Licensee MDPI, Basel, Switzerland. This article is an open access article distributed under the terms and conditions of the Creative Commons Attribution (CC BY) license (<https://creativecommons.org/licenses/by/4.0/>).

1. Introduction

The reuse and recycling of waste, whether industrial or agro-industrial, in cement materials, represents in many cases economic, technological and environmental advantages [1]. An example of solid waste generated in large quantities around the world is rubber waste from tires: this material is widely studied for applications in asphalt coatings [2], waterproofing [3], and as fillers in masonry mortars [4]. A study by [4] evaluated the feasibility effect of using fly ash and rubber wastes with Portland cement in mortars to coat masonry, concluding that mixes containing 10% Portland cement, 70%, and 60% fly ash and 20% and 30% of tire rubber particles showed technological properties suitable for masonry applications. Another study evaluated the production of controlled low-strength material without cement (CLSM) as a function of the pozzolanic reaction between the waste glass powder (GP) and hydrated lime (HL). In this study, the various mixes were technologically characterized as to their durability and microstructure, concluding that there is the possibility of applying, on a large scale, waste glass in the cement industry, promoting the sustainability of this production chain [5]. Another possibility of applying

glass waste is its addition as a finely ground powder in concrete, aiming at reducing the amount of cement and improving the internal filling of the matrix. Thus, [6] evaluated the effect of this addition on mechanical properties, water absorption, and durability in concrete, showing that the glass waste was beneficial in these applications, functioning as matrix filling.

The reinforcement of cementitious materials with fibers, whether natural or traditional, is the object of many studies that evaluated their technological properties, performance, and durability. Traditional fibers, such as glass, steel, and carbon, are used in order to improve flexural strength, as assessed by [7], who concluded that the use of glass fibers in mortars increased their flexural strength, as well as improved their fracture strength and ductility. A disadvantage of using fiberglass is the degradation resulting from the alkalinity of cementitious materials [8], which is also seen as a problem in the use of natural fibers without treatments [9]. Another study evaluated the use of other traditional fibers, such as basalt, which can help with durability in an alkaline environment but can represent high costs [10].

In the case of carbon fiber mortar reinforcement applications, they showed the ability to conduct electricity in mortars [11] and improve their performance against fire [12]. A great advantage of using natural fibers over traditional ones is its low cost of exploitation, due to its abundance, and lower energy consumption for its production, however, as a disadvantage there is the need for surface treatment to improve its durability in the cement matrix and great variability of its properties, depending on the type of fiber [12].

The wide diversity of natural fibers available in various parts of the world has contributed to the advancement of research on their reuse [13]. The applications of natural fibers can cover various types of filling matrices, such as ceramics [14], geopolymer [15], polymer [16], and Portland cement [17], behaving as a reinforcement material. Fiber-reinforced composites had their biggest development during and after the Second World War due to the great need to develop alternative materials with superior technological characteristics, such as greater lightness [18].

The introduction of the use of natural fibers, which can be extracted from different parts of a plant, revolutionized the textile [19] and composites industries for ballistic purposes [20], guaranteeing significant performance improvements. However, the civil construction sector has been requesting new materials, more environmental-friendly and advantageous in terms of performance [17]. Countries that have great agricultural potential, such as Brazil, generate huge amounts of fibers that are often discarded as waste after some processing process, as is the case with açai fibers [21].

Açai (*Euterpe oleracea*) is a typical fruit from the Amazon region, located in South America, which is used in cosmetics, medicines, and food industries, being widely consumed in Brazil and currently exported to several countries such as the United States and Canada [22]. During its beneficiation process, two agro-industrial wastes are generated—the lump (Figure 1a) and the fibers (Figure 1b)—which are disposed of in large volumes in landfills, generating financial costs for the industries.

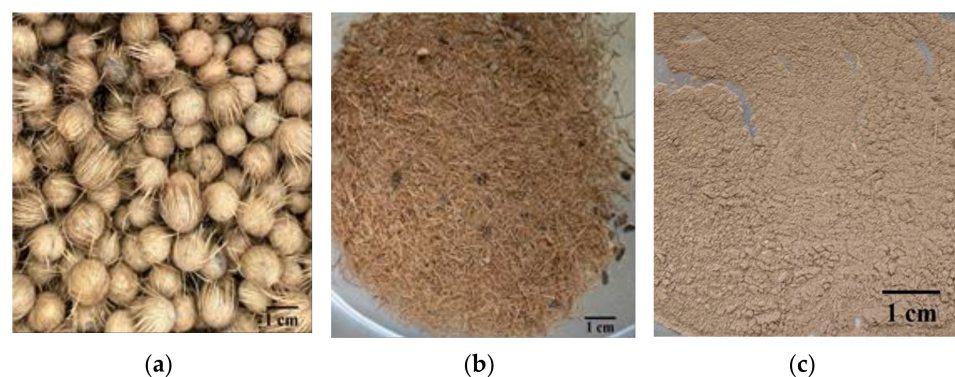


Figure 1. Açai waste: (a) Lump; (b) Natural açai fibers [23]; (c) Ground açai fibers.

Some research has been developed over the last few years aiming at the reuse of these wastes in the development of alternative construction materials. For example, Barbosa et al. [24] investigated the use of ground lump in ceramic matrices for the production of structural blocks, proving that up to 15% lump incorporation in traditional ceramic mass burned at 1050 °C produced blocks with high mechanical and physical properties, which can be applied for the development of more ecological and economical materials.

Azevedo et al. [25] evaluated the application of natural açai fibers in cement- and lime-based mortars, with addition ratios of 1.5%, 3.0%, and 5.0% by cement weight, both in natura (i.e., untreated) and treated with NaOH. In addition, the fibers were characterized regarding their physical, chemical, and morphological conditions, besides the fresh and hardened properties of the mortars [8]. The results revealed that additions of 3% of treated fibers provided good reinforcement in mortar, which is beneficial for its application in civil construction. However, such a study evidenced a usual problem of the application of natural fibers in cementitious matrices: their durability in high alkalinity medium (such as in Portland cement matrix) that can compromise the integrity of the composite. In this regard, Marvila et al. [26] evaluated issues and parameters related to the durability of mortars containing açai fibers, such as their exposure to wetting and drying cycles, salt spray, and thermal shock. The authors observed that the addition of the treated fibers mitigated the mechanical strength reduction after the different exposure cycles, corroborating its reinforcement purpose. In addition, 1.5% fiber incorporation resulted in the best overall performance.

The main studies of cementitious materials reinforced with natural fibers are intended to evaluate mechanical parameters, such as strength and durability, due to the effect that fibers usually have on this type of matrix [17,27]. In turn, studies focusing on the condition of the fluid paste, such as rheological behavior or even its interaction with the heat release throughout the cement hydration process, are still few in the literature of cement materials with additions of natural fibers [28]. The rheological parameters are essential to the knowledge of pastes and their behavior regarding workability, which is related to the casting capacity of the fresh mix and can affect its performance parameters in the hardened state [29]. The use of natural fibers can reduce the workability of pastes and mortars [30]; however, treating these fibers can lead to positive changes in the rheology and hydration of the cementitious matrix.

The objective of this work is an experimental investigation on the rheology, hydration, and microstructure of Portland cement pastes with the addition of açai fibers in different conditions (in natura and treated, in dry and saturated conditions), at different contents. It is noteworthy that because it is a fiber little explored in the literature, there are no consistent studies aimed at this type of addition in cementitious pastes.

2. Materials and Methods

2.1. Materials and Mixes

Ordinary Portland cement and deionized water were used in all mixes. Table 1 presents the chemical composition (obtained by X-ray fluorescence), the mineralogical composition (obtained by X-ray diffraction and Rietveld analysis, with R_{wp} of 7.4%), and the physical properties of the cement used. A quartz powder (>98 wt.% SiO₂) was used as an inert filler. Açai fibers were extracted from açai waste (Figure 1a). The waste was ground in a planetary ball mill (PULVERISETTE 6, Fritsch) for 30 min at 300 rpm with 10 agate balls of 10 mm in diameter, and then was sieved in a 150 µm-opening mash to separate the seeds from the fibers (Figure 1b). Then, the fibers were ground in the same ball mill for another 180 min to reach a powder-like size (Figure 1c). The fibers were used in four ways: in natura and chemically treated, each one in a dry and saturated condition. The chemical treatment was based on that adopted by Azevedo et al. [17]. For this purpose, about 10 g of fibers were immersed in 300 mL of a previously prepared NaOH solution (with 10 wt.% concentration) for 30 min while stirring. Then, the fibers were washed with distilled water and subsequently immersed in HCl solution (1:10 in volume) for another

30 min while stirring to neutralize the pH of the fibers. Finally, the fibers were washed with distilled water again and dried in an oven at 60 °C until reaching constant weight. For the saturated application, about 10 mg of fibers were immersed in 200 mL of water, homogenized, rested for 1 h, and then kept in a room at 23 °C and 50% relative humidity.

Table 1. Composition and properties of the Portland cement used.

Chemical Composition (%)		Physical Properties	
SiO ₂	18.87	Specific gravity (g/cm ³)	3.12
Al ₂ O ₃	4.29	Blaine fineness (m ² /kg)	447.4
Fe ₂ O ₃	2.97	28-day compressive strength (MPa)	51.2
CaO	58.92		
K ₂ O	0.85	Mineralogical Composition (wt.%)	
Na ₂ O	0.27	C3S	54.3
MgO	5.90	C2S	14.9
SO ₃	3.10	C3A	1.8
TiO ₂	0.63	C4AF	8.97
BaO	0.19	Calcite	10.1
PbO	<0.05	Dolomite	1.7
		Periclase	5.4
LOI	4.17	Gypsum	2.4

LOI: loss on ignition (CO₂)

Fourier-transform infrared spectroscopy (FTIR) was conducted using a Cary 600 Series (Agilent, Santa Clara, CA, United States) spectrometer, with an analysis range of 500–4000 cm⁻¹, resolution of 16 cm⁻¹, and 64 accumulations. X-ray diffraction (XRD) tests were conducted using a Miniflex II Desktop (Rigaku, Tokyo, Japan) diffractometer operating at 30 kV and 15 mA with CuK α radiation and wavelength of 1.5406 Å. Zeta potential tests were conducted using a Malvern Zetasizer Nano, at a size range of 3.8 nm–100 μ m, temperature of 25 °C, and pH of 7. SEM images of the fibers and the hydrated pastes were acquired using a VEGA3 (TESCAN) microscope operating at 15 kV. Energy-dispersive X-ray spectroscopy (EDS) analysis was also conducted in these samples using an x-art (Oxford) detector. The characterization results are presented in Section 3.1.

A total of nine cement pastes were prepared, with a constant water-to-solid ratio of 0.50 by weight. A reference (i.e., control) paste was produced containing only cement and distilled water, while the fibers replaced cement at 5% and 10% by weight. Fibers are usually incorporated in amounts related to the overall composite; however, since ground açai fibers were used here in a particle size distribution similar to that of a filler, they were classed in terms of cement replacement. Additionally, pastes with 5% and 10 wt.% replacement with inert quartz powder were produced. Table 2 details the composition of the pastes investigated, where the sample name is given by the content (5% and 10%) and type of fibers (“IN” for in natura, “T” for treated, and “S” for saturated) or quartz powder (QTZ), besides REF for the control mix. The percentages of addition of natural fiber were determined based on other studies in the literature [31,32].

Table 2. Detailed composition of the pastes investigated (in weight basis).

Mix	Cement	Fibers	Quartz Powder	Water	Description
REF	1.00	-	-	0.50	Plain cement paste
5 IN	0.95	0.05	-	0.50	5% dry in natura fibers addition
10 IN	0.90	0.10	-	0.50	10% dry in natura fibers addition
5 IN-S	0.95	0.05	-	0.50	5% saturated in natura fibers addition
10 IN-S	0.90	0.10	-	0.50	10% saturated in natura fibers addition
5 T	0.95	0.05	-	0.50	5% dry chemically-treated fibers addition
5 T-S	0.90	0.10	-	0.50	5% saturated chemically-treated fibers addition
5 QTZ	0.95	-	0.05	0.50	5% quartz powder addition
10 QTZ	0.90	-	0.10	0.50	10% quartz powder addition

The materials were mixed using a hand mixer (with 6000 rpm capacity) in batches of 15 mL. Firstly, the dry materials and water were added to the mixer container and mixed by hand for one minute. Then, the paste was mixed for 2 min.

2.2. Experimental Procedures

The rheological tests were conducted using a Haake MARS III (Thermo Fisher Scientific, Waltham, MA, USA) rheometer equipped with a parallel-plate geometry with a hatched surface to prevent wall slip. The geometry diameter and the axial gap were 35.00 and 1.00 mm, respectively, and the temperature was kept at 23.0 ± 0.1 °C. The rheological tests started 10 min after the first contact between the dry materials and water. The flow curves were obtained by increasing the shear rate from 0.1 to 100 s^{-1} in 10 steps and subsequently decreasing it down to 0.1 s^{-1} in the same steps. In each step, the shear rate was kept for 30 s (which was enough to reach a steady-state flow), and the final 3 s of each step were recorded. The rheological properties, i.e., yield stress τ_0 (in Pa) and viscosity μ (in Pa.s), were determined using Equations (1) and (2) respectively, where τ is the shear stress (in Pa), $\dot{\gamma}$ the shear rate (in s^{-1}), K and n the consistency and pseudoplastic parameters of the Herschel-Bulkley model, and $\dot{\gamma}_{\max}$ the maximum shear rate applied (in s^{-1}).

$$\tau = \tau_0 + K \cdot \dot{\gamma}^n \quad (1)$$

$$\mu = \frac{3K}{n+2} \cdot (\dot{\gamma}_{\max})^{n-1} \quad (2)$$

The cement hydration kinetics was evaluated through isothermal calorimetry, conducted using a TAM Air (TA Instruments) calorimeter at 23 °C. Immediately after mixing, about 10 g of fresh paste was placed into the calorimeter container, and the heat release was recorded for up to 160 h. The calorimetry results (i.e., the heat flow and cumulative heat) were normalized for the weight of dry material. After the calorimetry test, the samples were removed from the container, ground until passing through a 75 μm -opening mesh, and immediately tested through XRD under the testing conditions detailed in Section 2.1. At this age, a broken piece of paste was also analyzed through SEM using the equipment and conditions detailed in Section 2.1.

3. Results and Discussion

3.1. Fiber Characterization

Figure 2a shows the FTIR spectra of in natura and treated açai fibers. The broad band at $3600\text{--}3200 \text{ cm}^{-1}$ is associated with the O–H stretching of both lignin and cellulose: while the band attributed to lignin is placed around 3560 cm^{-1} , those associated with cellulose are placed at around $3280\text{--}3220 \text{ cm}^{-1}$ [33]. The band at 2920 cm^{-1} is associated with C–H stretching of methyl and methylene groups of cellulose [33,34]. The 1735 cm^{-1} band is associated with C=O carboxyl and acetyl groups from (hemi)cellulose and the 1619 cm^{-1} band is associated with C=C stretching of groups in lignin [34]. The bands at 1380 and 1045 cm^{-1} are associated with stretching vibrations of different carbohydrate groups, and the band at 1253 cm^{-1} is associated with C–O stretching of lignin [33]. Figure 2b presents the XRD patterns of in natura and treated açai fibers. Both fibers showed a broad peak at around $22.1^\circ 2\theta$ associated with the combined amorphous contribution of lignin [35] and cellulose [36], in addition to minor peaks at 16.8 and $34.3^\circ 2\theta$ associated with the latter.

It is worth noting that lignin removal with alkaline treatment has already been reported in the literature. Wunna et al. [37] treated sugarcane bagasse with 0.5–2.0% of NaOH for 10–120 min for this purpose. Popescu [38] partially removed lignin from Eucalyptus and Norway spruce woods with 0.3% NaOH for 1 h. In turn, acid treatment is known for promoting cellulose hydrolysis [39], as observed by Dagnino et al. [40] when treated rice hulls with 0.3–2.4% H_2SO_4 solution for 33 min. Considering that a coupled treatment with NaOH and HCl was used in this work, it can affect both lignin and cellulose from the açai fibers. The FTIR results revealed that the chemical treatment reduced the bands at $3280\text{--}3220$, 2920 , 1735 , and 1253 cm^{-1} associated with cellulose, while evidenced the

“shoulder” band at 3560 cm^{-1} and kept the band at 1619 cm^{-1} associated with lignin. These results indicate a cellulose removal with the treatment while no major changes in lignin content seem to have occurred. As for the XRD results, the chemical treatment narrowed the main diffuse peak at $22.1^\circ 2\theta$, while evidencing two minor peaks at about 16.8° and $34.3^\circ 2\theta$. It is stressed that XRD evaluates the long-range order (i.e., the crystalline structure) of the material, while spectroscopy techniques (such as FTIR and Raman) evaluate the local order of the material on the scale of atomic bonds [41,42]. Thus, XRD suggests that the chemical treatment disrupted the long-range order of lignin structure, but apparently without substantially reducing its content (from FTIR results).

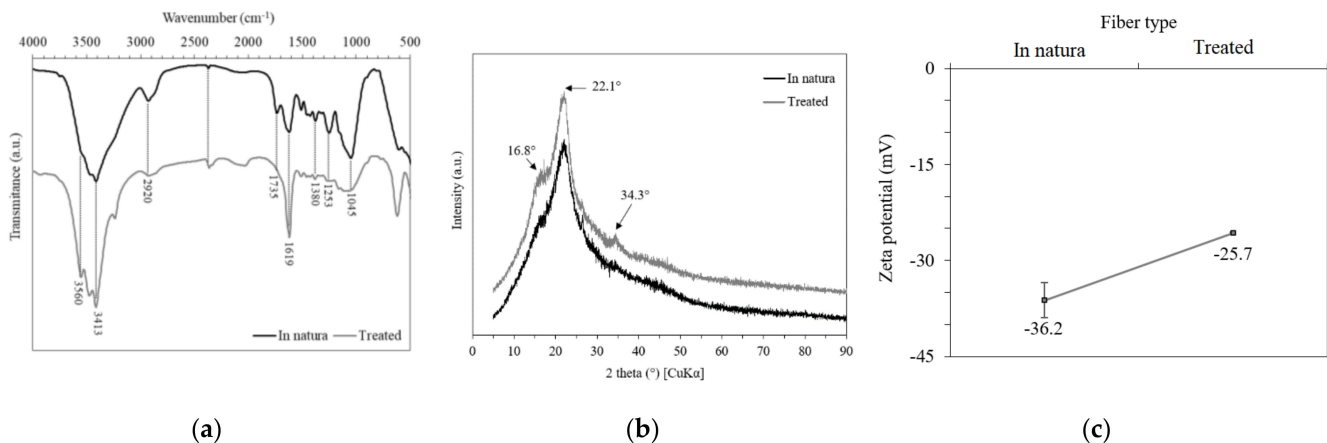


Figure 2. Characterization of the açai fibers. (a) FTIR spectra; (b) XRD patterns; (c) Zeta potential (average \pm standard deviation of three measurements).

Figure 2c shows the zeta potential of the fibers before and after the treatment. The chemical treatment reduced the absolute zeta potential value from -36.2 to -25.7 mV, indicating an increased agglomeration trend with the chemical treatment.

Figure 3 shows the SEM-EDS results of the açai fibers characterization. The EDS results correspond to the average wt.% and standard deviation of 6–8 area measurements randomly selected, while one representative spectrum is shown for each sample. The chemical treatment made the fiber surface less smooth, increasing its roughness on a scale of a few micrometers (Figure 3b,e). In addition, the EDS results showed that the carbon content was significantly reduced (from 75.3 to 60.4 wt.% on average) with the chemical treatment. These trends can be attributed to lignin and cellulose removal.

3.2. Rheological Tests

Figure 4 shows the flow curves (i.e., shear stress vs. shear rate) of the pastes. The flow curves can be divided into two groups: the REF mix, the mixes containing 5% of either fiber and the mixes with 5% and 10% quartz powder (marked a) presented shear stresses within 10–90 Pa, while the mixes containing 10% of either fiber (marked b) showed significantly higher shear stresses, within 180–600 Pa. In addition, two flow curve profiles can be noted. In the (a) group, viscosity (visually assessed by the slope of the flow curve) was approximately constant at low shear rates (marked (i) in Figure 4), followed by a shear thickening region (marked (ii)) that is characterized by an increase in viscosity as the shear rate increases. In contrast, the mixes of the (b) group showed a shear-thinning response at low shear rates (marked (iii)) that corresponds to a viscosity decrease with the shear rate increase, followed by a shear thinning behavior at higher shear rates as for (a) group. The shear thickening response at high shear rates has already been reported for cement-based materials [43–46]. This corresponds to the transition from a shear-ordered structure (e.g., in (i)) to a state of hydrodynamic clustering: as the shear rate increases, the hydrodynamic forces become enough to remove the particles from the layer-like flow, disturbing the ordered state and consequently clustering the particles [47]. Since these

clusters are formed by hydrodynamic forces, this phenomenon is ended with a decrease in the flow rate [45].

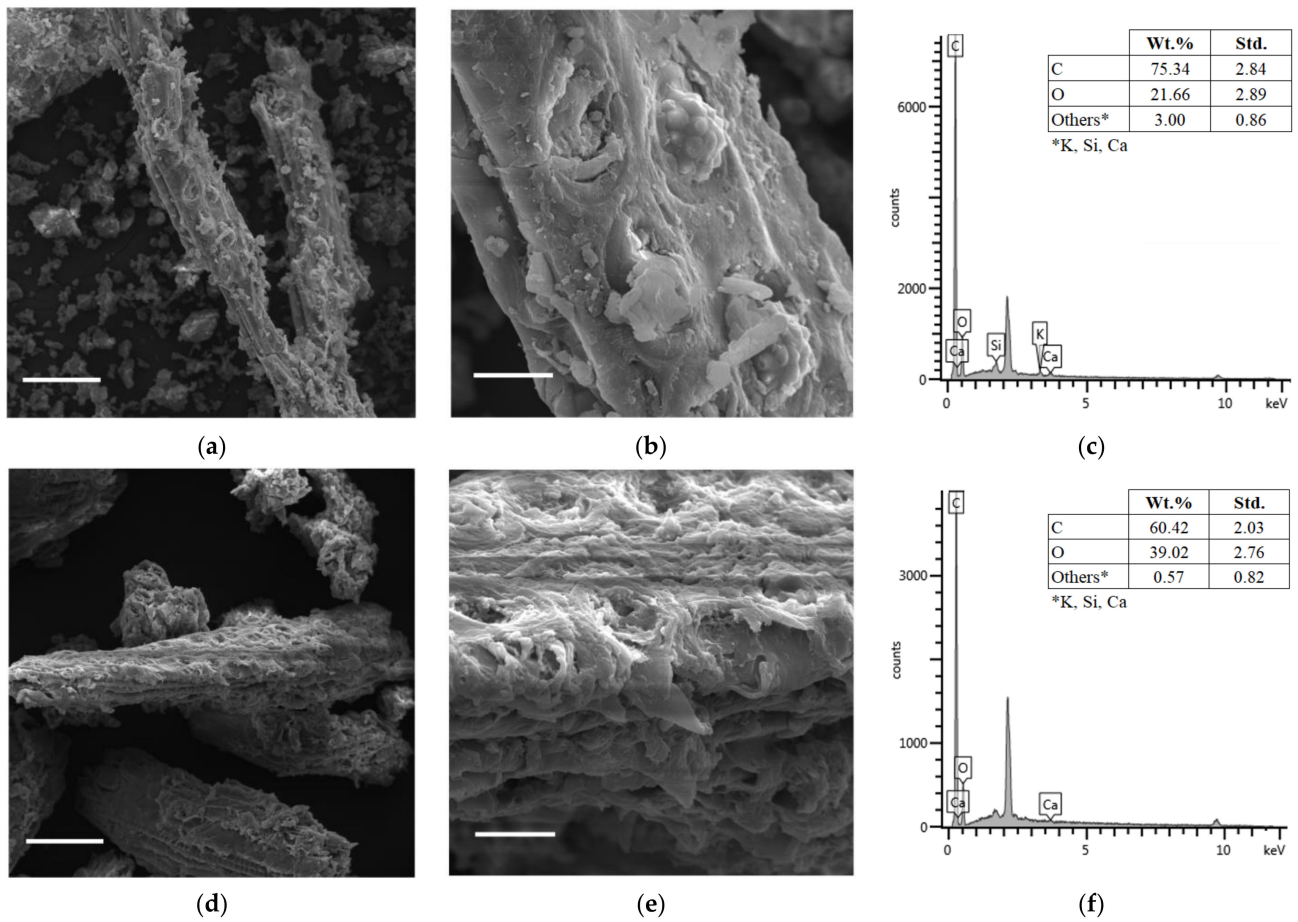


Figure 3. SEM-EDS results of the açai fibers. In natura: (a) [$\times 1000$; scale = 50 μm]; (b) [$\times 5000$; scale = 10 μm]; (c) EDS spectrum. Treated: (d) [$\times 1000$; scale = 50 μm]; (e) [$\times 5000$; scale = 10 μm]; (f): EDS spectrum.

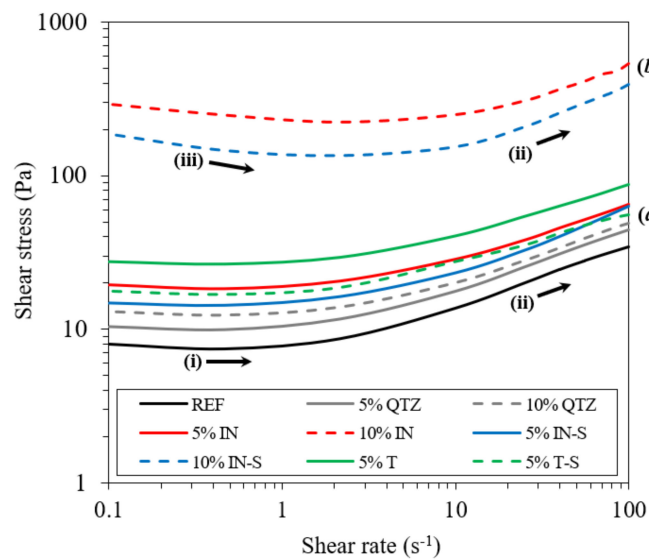


Figure 4. Flow curves of the pastes. Note: IN = in natura, S = saturated; T = treated; QTZ = quartz.

In turn, the shear-thinning response at low shear rates for the (b) group may be associated with two phenomena. The increasing shear rate can release the water absorbed by the fibers during mixing (for dry fibers) or previously added (for saturated fibers). The occurrence of water release with shearing was previously reported by Mechtcherine et al. [48] for cement mortar containing superabsorbent polymers (SAP). Also, the fibers that are initially randomly oriented can align with the increasing shear, facilitating the flow and thus reducing viscosity.

Figure 5 shows the rheological properties of the pastes. The incorporation of 5% of either replacement material increased the yield stress of the paste from 6.2 Pa (REF) to 24.3 Pa (5% T) and its viscosity from 0.3 Pa.s (REF) to 0.8 Pa.s (5% T). In turn, the incorporation of 10% fibers drastically improved the rheological properties of the paste, reaching a yield stress of 250 Pa and a viscosity of 2.8 Pa.s for the mix with 10% in natura fibers. This can be associated with the elongated shape of the fibers (Figure 3a,d), which hinders the flow of cement particles during shear. These results are consistent with those reported by Gwon and Shin [49], which incorporated 0–2% of cellulose microfibers in cement paste and observed progressive yield stress increases with the increase in fiber content. Moreover, for the same addition ratio, incorporating treated fibers slightly increased the yield stress of paste compared to the in natura fibers: 24.3 Pa for 5% T vs. 17.1 Pa for 5% IN, and 14.8 Pa for 5% T-S vs. 13.5 Pa for 5% IN-S. This can be associated with the partial removal of cellulose and the structural order disruption of lignin promoted by the chemical treatment, as per the FTIR and XRD results (Figure 2a,b). Lignin is one of the main constituents of lignosulphonate-based plasticizer admixtures, which promotes the dispersion of cement particles through electrostatic repulsion [50]. Montes et al. [51] found that cellulose nanocrystals can act like water-reducing agents by adsorbing on cement surfaces and improving the dispersion of the particles. Thus, the removal/disruption of these compounds may negatively affect the rheology of the fresh paste. Furthermore, the zeta potential results (Figure 2c) showed that the chemical treatment decreased its absolute value from -32.2 to -25.7 mV, indicating a higher agglomeration trend (and consequently worse dispersion) for the treated fibers, which can negatively impact the rheological properties of the cementitious composite. Finally, the rougher surface of the chemically treated fibers (Figure 3e) tends to increase the friction between the particles during flow, which can also hinder the rheological properties of the fresh mix.

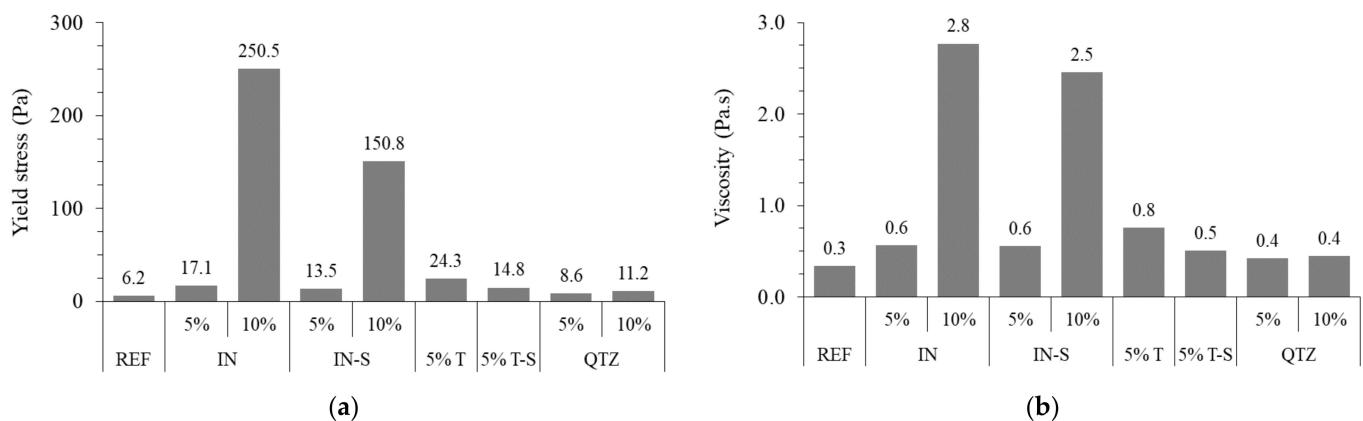


Figure 5. Rheological properties of the pastes: (a) yield stress; (b) viscosity. Note: IN = in natura, S = saturated; T = treated; QTZ = quartz.

Furthermore, dry fibers (both in natura and treated) led to further increases in yield stress and viscosity than the respective saturated fibers for the same incorporation level. This can be justified by the water absorption of the dry fibers: since both yield stress and viscosity are directly related to the inter-particle distance, the partial removal of mixing water caused by absorption increases the friction and probability of collision between particles. This behavior had already been reported in the literature for other absorbing

materials. Liu et al. [52] incorporated dry and pre-saturated SAP in ultra-high performance concrete, observing that the incorporation of pre-saturated SAP had a marginal effect on the yield stress and viscosity of concrete while the incorporation of dry SAP significantly affected it. Mechtcherine et al. [48] investigated the use of four types of SAP in cement mortar, finding that the water uptake by SAP was the major factor that governed the rheological properties of fresh mortar.

Finally, the incorporation of quartz powder also increased the yield stress and viscosity of the paste. These results are in agreement with those previously reported by Cyr et al. [53] and de Matos et al. [54] for quartz filler incorporation, and de Matos for other mineral fillers [55].

3.3. Hydration and Microstructure

Figure 6 presents the isothermal calorimetry curves of the pastes. Incorporating 5% of either in natura fiber delayed the occurrence of the main heat flow peak from 11.3 h (REF) up to 71.8 and 75.5 h, respectively, for 5% IN and 5% IN-S. In turn, the incorporation of 10% of either in natura fiber (10% IN and 10% IN-S) delayed the main heat flow peak for over 160 h, which was the maximum testing time. De Lima et al. [56] characterized açai fibers, observing that they are usually composed of about 9% moisture, 2% incombustible (i.e., ash), and 89% volatile matter, the latter corresponding mainly to sugars. The volatile fraction was composed of 30% glucose, 19% xylose, 45% polysaccharides (27% cellulose + 18% hemicellulose), and 35% lignin. In this regard, Kochova et al. [57] investigated the effect of different saccharides on the hydration of cement pastes. The authors observed that the addition of 0.2% and 0.5% glucose delayed the main heat flow peak by about 2 and 5 days, respectively, compared with plain cement paste; 0.2% sucrose addition was enough to delay it for 5 days. According to these authors, saccharides change the surface of the hydrating cement particles and hydration products, promoting the formation of a temporary barrier and therefore hindering further reaction. In addition, the authors observed that the increase in saccharide content reduces the concentration of Ca^{2+} ions in pore solution. It is well accepted that the Ca^{2+} supersaturation (and consequent precipitation of $\text{Ca}(\text{OH})_2$) is the trigger for the main cement reactions [58,59]. Thus, a reduction in the Ca^{2+} concentration delays cement's hydration kinetics. Similar trends were reported when different natural microfibers were added to the cementitious paste. Gwon et al. [60] incorporated 0.3–2.0% of cellulose microfiber over the cement weight in paste, observing that the main heat flow peak delayed from 16.6 h (control mix) up to 28.9 h (2% fiber). Delannoy et al. [61] incorporated ground hemp shives in 1–10% over the cement weight, observing that 5% addition delayed the main peak of heat release by 24 h, while 10% addition delayed it by over 144 h (the maximum testing time), similarly to that observed in the current work. One can expect that the reduction in the cement content caused by its replacement would delay the hydration due to the lower release of Ca^{2+} ions in the pore solution. However, the incorporation of the quartz inert filler did not significantly affect the occurrence of the main heat flow peak for either replacement levels, indicating that the delay observed in the mixes with the fibers was not related with the cement reduction.

The chemical treatment considerably reduced the delay in cement hydration caused by açai fiber incorporation, leading to the occurrence of the main hydration peak at 14.2 h when either treated fibers were added at 5% (5% T and 5% S, Figure 6a). This behavior can be attributed to the reduction in lignin and cellulose contents discussed in Section 3.1. In addition, isothermal calorimetry curves showed that the hydration kinetics of pastes with 5% of either treated fibers was slower than that of plain cement paste within the first days (Figure 6a) but practically matched its cumulative heat at 160 h (with a difference of 2.8%, Figure 6b). These results indicate that the combined NaOH/HCl treatment used was effective in reducing the delay in cement hydration caused by açai fiber incorporation.

Figure 7 shows the XRD patterns of the hydrated pastes at 160 h. Regarding the mixes with açai fibers, the incorporation of 5% in natura fibers led to low portlandite (18.1, 34.1

and $47.1^\circ 2\theta$) and ettringite ($8.9, 15.8$ and $23.0^\circ 2\theta$) peak appearances, while the main alite peaks ($29.3, 32.1, 41.2$ and $51.7^\circ 2\theta$) were much more intense than in the other samples. This indicates the lower consumption of the main clinker phase (alite) and the lower formation of hydrated products (portlandite and ettringite) at this age. Such behavior is explained by the delay in the cement hydration caused by the incorporation of in natura fibers, identified by the calorimetry results. In contrast, the incorporation of 5% treated fibers (5% T) led to a similar XRD pattern than plain cement paste did, in agreement with their close 160 h cumulative heat results in calorimetry (Figure 6b). This was also found for the 5% QTZ mix, in line with the calorimetry results. Finally, the calcite ($39.2^\circ 2\theta$) and periclase ($42.9^\circ 2\theta$) peaks were similar for all the mixes since these phases were not consumed, while the 5% QTZ mix showed additional reflections at 23.6 and $36.6^\circ 2\theta$ attributed to quartz.

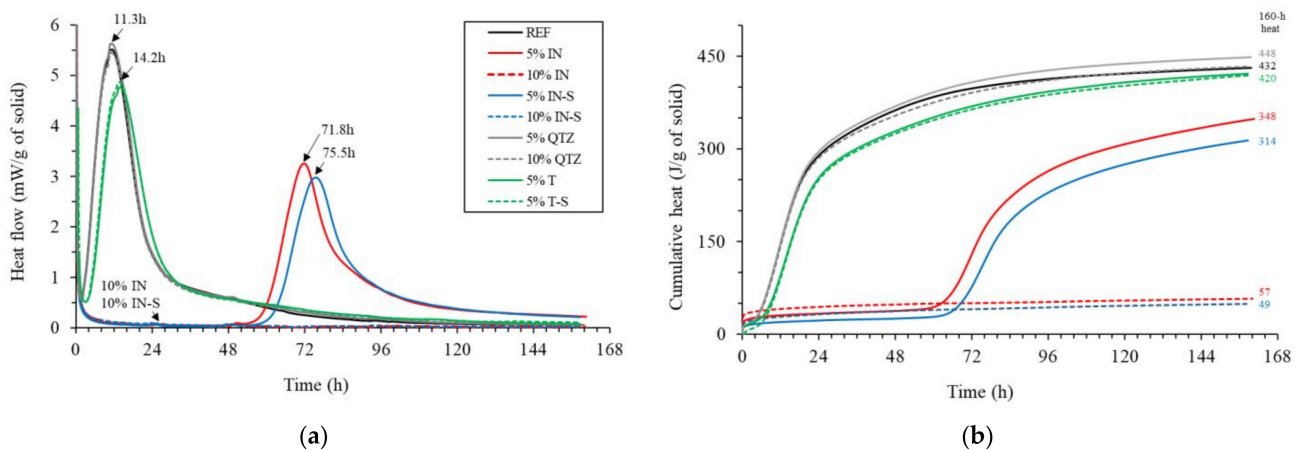


Figure 6. Isothermal calorimetry curves of the pastes up to 160 h: (a) heat flow; (b) cumulative heat. Note: IN = in natura, S = saturated; T = treated; QTZ = quartz.

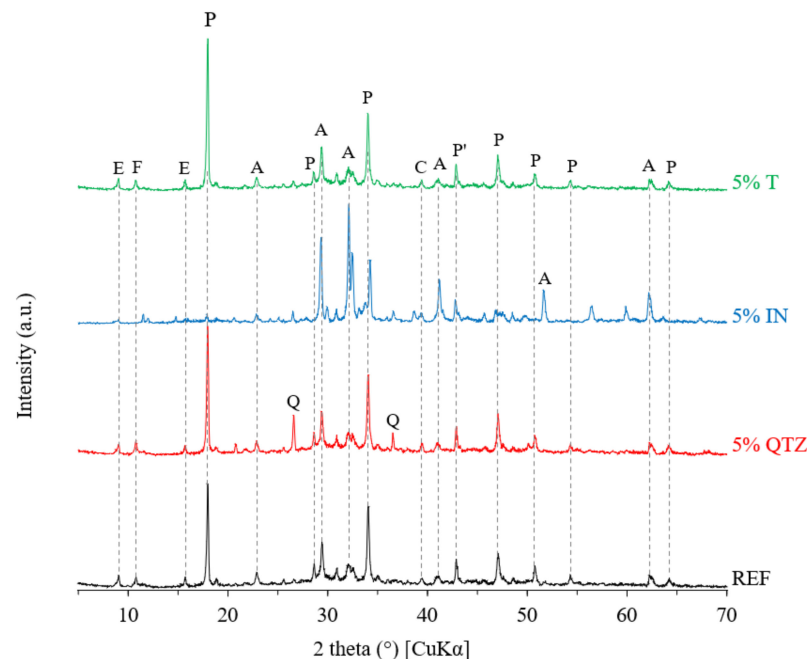


Figure 7. XRD pattern of the pastes at 160 h of hydration. A: alite; C: calcite; E: ettringite; F: ferrite; P: portlandite; P': periclase; Q: quartz.

Figure 8 shows SEM images of the hydrated pastes at 7 days. The cementitious matrix of the REF mix was dense with few pores (Figure 8a,b), while the fibers incorporation visually increased its macroporosity (Figure 8c,d), as evidenced by the presence of several voids in the scale of a few tens of micrometers. The increased air content of cementitious

composite with lignin-based admixture incorporation is well documented in the literature [50]. In addition, the fiber incorporation reduced the flowability (i.e., increased the yield stress and viscosity) of the paste, which can prevent the air from leaving the mix during the fresh state. [62,63]. Nonetheless, for further conclusions on porosity, additional characterization is needed (e.g., by mercury intrusion porosimetry).

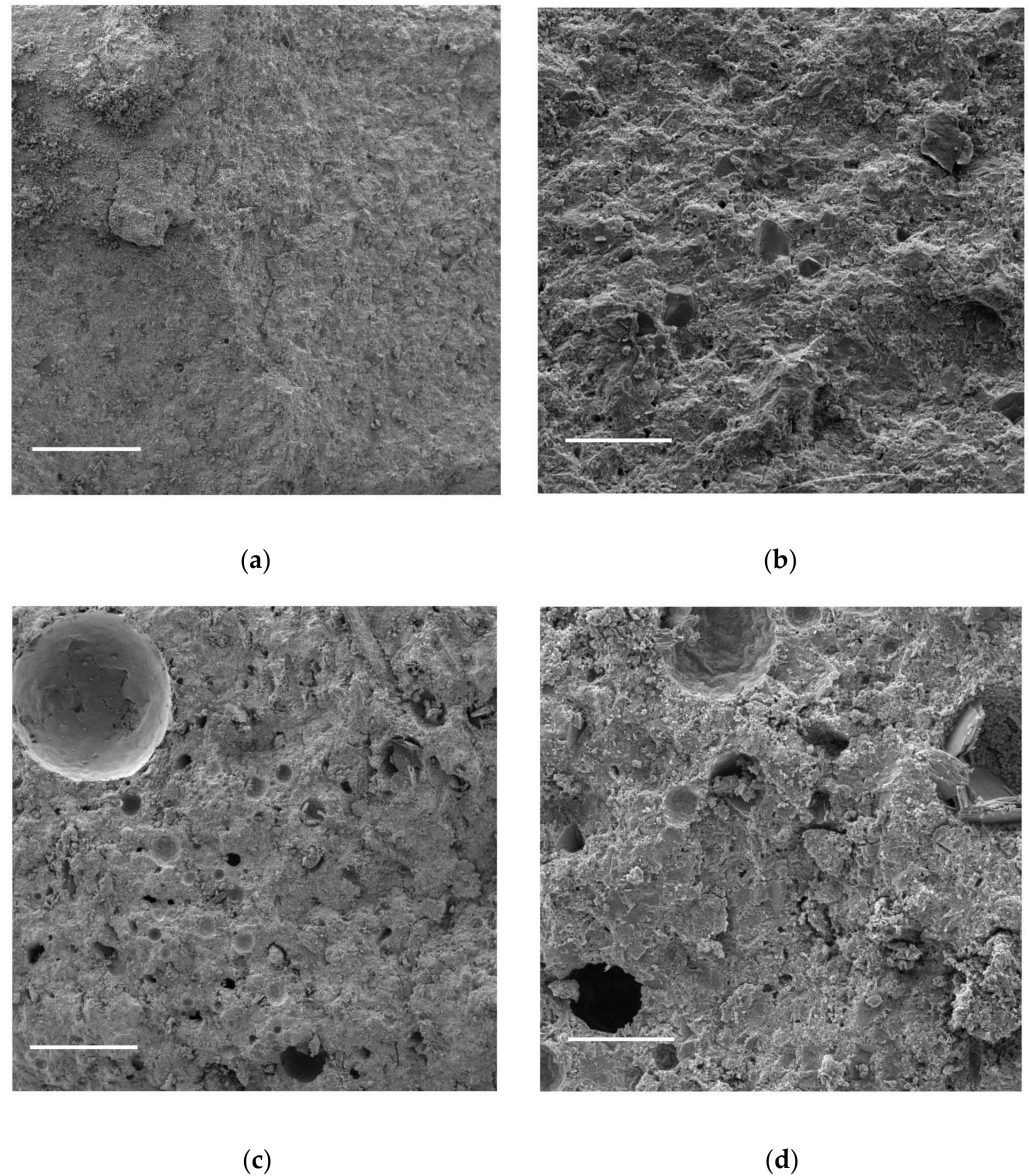


Figure 8. SEM images of the pastes at 7 days of hydration. REF: (a) [$\times 100$; scale = 500 μm]; (b) [$\times 500$; scale = 100 μm]. 5% T: (c) [$\times 100$; scale = 500 μm]; (d) [$\times 500$; scale = 100 μm].

4. Conclusions

This work investigated the effect of açai ground fiber incorporation on the rheology, hydration, and microstructure of Portland cement pastes. In natura and chemically treated (with NaOH and HCl) fibers were used, in dry and saturated conditions. The FTIR, XRD, and SEM-EDS results revealed that the chemical treatment reduced the cellulose and lignin contents in açai fibers while increasing their surface roughness. The treatment also reduced the zeta potential (in absolute value), increasing the agglomeration trend.

When incorporated in cement paste, 5% addition of either fiber slightly increased the yield stress and viscosity of the paste, while 10% addition drastically increased these properties, reaching yield stress and viscosity values respectively 40 and 8 times higher

than those of plain paste. The highest incorporation level led to shear-thinning response at low shear rates, probably associated with the water release and fiber alignment with the increasing shear rate.

The incorporation of 5% in natura fibers delayed the cement hydration kinetics by about 2.5 days while 10% in natura fibers delayed it by over 160 h, which was the maximum testing time. In contrast, the chemical treatment significantly reduced this retarding effect, leading to a 3 h delay when 5% treated fibers were incorporated. At 160 h, in natura fibers significantly reduced the cumulative heat (314–348 J/g compared with 432 J/g for plain paste), while the chemical treatment led to a 420 J/g cumulative heat at this age. In line with these results, XRD measurements at 160 h of hydrated pastes revealed comparable compositions for both plain and 5% treated fiber pastes, while the paste with 5% in natura fibers had lower alite consumption and low hydrates (i.e., portlandite and ettringite) formation. SEM of 7-day-old pastes revealed that the incorporation of açai fibers increased the macroporosity of the cementitious matrix.

Overall, the combined NaOH/HCl treatment was effective for açai fiber functionalization, and the incorporation of 5% treated fibers led to fresh and hardened performances comparable to those of plain cement paste, indicating the feasibility of using such fibers in cementitious composites. As a general requirement to be used as reinforcement in a cementitious matrix, natural fibers should have a proper surface chemical composition (even if it requires chemical treatment), with controlled contents of lignin and cellulose.

Author Contributions: Conceptualization, A.A. and M.M.; methodology, A.A. and P.d.M.; validation, R.S.; formal analysis, L.S.; investigation, R.S., and L.S.; resources, P.G.; data curation, P.d.M. and L.S.; writing—original draft preparation, A.A., P.d.M. and M.M.; writing—review and editing, P.G. and J.d.B.; supervision, P.G., and J.d.B.; funding acquisition, P.G., and J.d.B. All authors have read and agreed to the published version of the manuscript.

Funding: This research received no external funding.

Acknowledgments: A.A. acknowledges the Brazilian governmental agencies CAPES, CNPq, and FAPERJ (proc. number E-26/210.150/2019) for their financial support. P.d.M., R.S., L.S., and P.G. acknowledge the Brazilian governmental agencies CAPES, CNPq, and FAPESC for their financial support. LabMat-UFSC and Patrícia Prates are kindly acknowledged for the SEM-EDS analysis. J.d.B. acknowledges the support of Instituto Superior Técnico, the CERIS research unit, and the Foundation for Science and Technology.

Conflicts of Interest: The authors declare no conflict of interest.

References

1. Cho, B.H.; Nam, B.H.; An, J.; Youn, H. Municipal Solid Waste Incineration (MSWI) Ashes as Construction Materials—A Review. *Materials* **2020**, *13*, 3143. [[CrossRef](#)]
2. Nabil, K.; Farid, B.; Ali, Z. Valorization of asphalt rubber fine powder in road field. In Proceedings of the Key Engineering Materials, Kota Kinabalu, Malaysia, 8–9 March 2013.
3. Wang, R.; Gao, P.; Tian, M.; Dai, Y. Experimental study on mechanical and waterproof performance of lightweight foamed concrete mixed with crumb rubber. *Constr. Build. Mater.* **2019**, *209*, 655–664. [[CrossRef](#)]
4. Yilmaz, A.; Degirmenci, N. Possibility of using waste tire rubber and fly ash with Portland cement as construction materials. *Waste Manag.* **2009**, *29*, 1541–1546. [[CrossRef](#)]
5. Xiao, R.; Polaczyk, P.; Jiang, X.; Zhang, M.; Wang, Y.; Huang, B. Cementless controlled low-strength material (CLSM) based on waste glass powder and hydrated lime: Synthesis, characterization and thermodynamic simulation. *Constr. Build. Mater.* **2021**, *275*, 122157. [[CrossRef](#)]
6. Jurczak, R.; Szmatała, F.; Rudnicki, T.; Korentz, J. Effect of Ground Waste Glass Addition on the Strength and Durability of Low Strength Concrete Mixes. *Materials* **2021**, *14*, 190. [[CrossRef](#)] [[PubMed](#)]
7. Keleştemur, O.; Yildiz, S.; Gökçer, B.; Arici, E. Statistical analysis for freeze–thaw resistance of cement mortars containing marble dust and glass fiber. *Mater. Des.* **2014**, *60*, 548–555. [[CrossRef](#)]
8. Purnell, P.; Short, N.R.; Page, C.L. A static fatigue model for the durability of glass fibre reinforced cement. *J. Mater. Sci.* **2001**, *36*, 5385–5390. [[CrossRef](#)]
9. De Azevedo, A.R.G.; Marvila, M.T.; Antunes, M.L.P.; Rangel, E.C.; Fediuk, R. Technological Perspective for Use the Natural Pineapple Fiber in Mortar to Repair Structures. *Waste Biomass Valorization* **2021**, 1–15. [[CrossRef](#)]

10. Fenu, L.; Forni, D.; Cadoni, E. Dynamic behaviour of cement mortars reinforced with glass and basalt fibres. *Compos. Part B Eng.* **2016**, *92*, 142–150. [[CrossRef](#)]
11. Hou, Z.; Li, Z.; Wang, J. Electrical conductivity of the carbon fiber conductive concrete. *J. Wuhan Univ. Technol. Sci. Ed.* **2007**, *22*, 346–349. [[CrossRef](#)]
12. Barrios, A.M.; Vega, D.F.; Martínez, P.S.; Atanes-Sánchez, E.; Fernández, C.M. Study of the properties of lime and cement mortars made from recycled ceramic aggregate and reinforced with fibers. *J. Build. Eng.* **2020**, *35*, 102097. [[CrossRef](#)]
13. Ferrara, G.; Pepe, M.; Martinelli, E.; Filho, R.D.T. Influence of an Impregnation Treatment on the Morphology and Mechanical Behaviour of Flax Yarns Embedded in Hydraulic Lime Mortar. *Fibers* **2019**, *7*, 30. [[CrossRef](#)]
14. Tassew, S.; Lubell, A. Mechanical properties of glass fiber reinforced ceramic concrete. *Constr. Build. Mater.* **2014**, *51*, 215–224. [[CrossRef](#)]
15. Malenab, R.A.J.; Ngo, J.P.S.; Promentilla, M.A.B. Chemical Treatment of Waste Abaca for Natural Fiber-Reinforced Geopolymer Composite. *Materials* **2017**, *10*, 579. [[CrossRef](#)] [[PubMed](#)]
16. Verma, D.; Senal, I. Natural fiber-reinforced polymer composites. In *Biomass, Biopolymer-Based Materials, and Bioenergy*; Elsevier: Amsterdam, The Netherlands, 2019; pp. 103–122.
17. De Azevedo, A.R.G.; Klyuev, S.; Marvila, M.T.; Vatin, N.; Alfimova, N.; de Lima, T.E.S.; Fediuk, R.; Olisov, A. Investigation of the Potential Use of Curauá Fiber for Reinforcing Mortars. *Fibers* **2020**, *8*, 69. [[CrossRef](#)]
18. Chaudhary, V.; Bajpai, P.K.; Maheshwari, S. Effect of moisture absorption on the mechanical performance of natural fiber reinforced woven hybrid bio-composites. *J. Nat. Fibers* **2020**, *17*, 84–100. [[CrossRef](#)]
19. Stanton, T.; Johnson, M.; Nathanael, P.; MacNaughtan, W.; Gomes, R.L. Freshwater and airborne textile fibre populations are dominated by ‘natural’, not microplastic, fibres. *Sci. Total Environ.* **2019**, *666*, 377–389. [[CrossRef](#)]
20. Pereira, A.C.; de Assis, F.S.; Filho, F.D.C.G.; Oliveira, M.S.; Demosthenes, L.C.D.C.; Lopera, H.A.C.; Monteiro, S.N. Ballistic performance of multilayered armor with intermediate polyester composite reinforced with fique natural fabric and fibers. *J. Mater. Res. Technol.* **2019**, *8*, 4221–4226. [[CrossRef](#)]
21. Santos, N.S.; Silva, M.R.; Alves, J.L. Reinforcement of a biopolymer matrix by lignocellulosic agro-waste. *Procedia Eng.* **2017**, *200*, 422–427. [[CrossRef](#)]
22. Ferreira, D.S.; Gomes, A.L.; Da Silva, M.G.; Alves, A.B.; Agnol, W.H.D.; Ferrari, R.A.; Carvalho, P.R.N.; Pacheco, M.T.B. Antioxidant Capacity and Chemical Characterization of Açai (*Euterpe oleracea* Mart.) Fruit Fractions. *Food Sci. Technol.* **2016**, *4*, 95–102. [[CrossRef](#)]
23. Azevedo, A.R.G.; Marvila, M.T.; Zanelato, E.B.; Lima, T.E.S.; Cecchin, D.; Souza, J.S.; Barbosa, M.Z.; Monteiro, S.N.; Rocha, H.A.; Alexandre, J.; et al. Evaluation of Different Methods of Surface Treatment of Natural Açai Fiber Added in Cementitious Composites. In *Characterization of Minerals, Metals, and Materials 2021. The Minerals, Metals & Materials Series*; Springer: Cham, Switzerland, 2021; pp. 383–391. [[CrossRef](#)]
24. Barbosa, A.D.M.; Rebelo, V.S.M.; Martorano, L.G.; Giaccon, V.M. Caracterização de partículas de açai visando seu potencial uso na construção civil. *Matéria* **2019**, *24*. [[CrossRef](#)]
25. De Azevedo, A.R.; Marvila, M.T.; Tayeh, B.A.; Cecchin, D.; Pereira, A.C.; Monteiro, S.N. Technological performance of açai natural fibre reinforced cement-based mortars. *J. Build. Eng.* **2021**, *33*, 101675. [[CrossRef](#)]
26. Marvila, M.T.; Azevedo, A.R.; Cecchin, D.; Costa, J.M.; Xavier, G.C.; Carmo, D.D.F.D.; Monteiro, S.N. Durability of coating mortars containing açai fibers. *Case Stud. Constr. Mater.* **2020**, *13*, e00406. [[CrossRef](#)]
27. Neruba, L.; Junio, R.F.; Ribeiro, M.P.; Souza, A.T.; Lima, E.S.; Garcia Filho, F.C.; Figueiredo, A.B.S.; Braga, F.O.; Azevedo, A.R.G.; Monteiro, S.N. Promising Mechanical, Thermal, and Ballistic Properties of Novel Epoxy Composites Reinforced with *Cyperus malaccensis* Sedge Fiber. *Polymers* **2020**, *12*, 1776. [[CrossRef](#)]
28. Bellotto, M. Cement paste prior to setting: A rheological approach. *Cem. Concr. Res.* **2013**, *52*, 161–168. [[CrossRef](#)]
29. De Matos, P.R.; Pilar, R.; Casagrande, C.A.; Gleize, P.J.P.; Pelisser, F. Comparison between methods for determining the yield stress of cement pastes. *J. Braz. Soc. Mech. Sci. Eng.* **2019**, *42*, 24. [[CrossRef](#)]
30. Aprianti, E.; Shafiqh, P.; Bahri, S.; Farahani, J.N. Supplementary cementitious materials origin from agricultural wastes—A review. *Constr. Build. Mater.* **2015**, *74*, 176–187. [[CrossRef](#)]
31. Quiñones-Bolaños, E.; Gómez-Oviedo, M.; Mouthon-Bello, J.; Sierra-Vitola, L.; Berardi, U.; Bustillo-Lecompte, C. Potential use of coconut fibre modified mortars to enhance thermal comfort in low-income housing. *J. Environ. Manag.* **2021**, *277*, 111–128. [[CrossRef](#)] [[PubMed](#)]
32. Azevedo, A.R.; Marvila, M.T.; Zanelato, E.B.; Alexandre, J.; Xavier, G.C.; Cecchin, D. Development of mortar for laying and coating with pineapple fibers. *Rev. Bras. Eng. Agrícola Ambient.* **2020**, *24*, 187–193. [[CrossRef](#)]
33. Poletto, M.; Zattera, A.J.; Santana, R.M.C. Structural differences between wood species: Evidence from chemical composition, FTIR spectroscopy, and thermogravimetric analysis. *J. Appl. Polym. Sci.* **2012**, *126*, E337–E344. [[CrossRef](#)]
34. Poletto, M.; Ornaghi, J.H.L.; Zattera, A.J. Native Cellulose: Structure, Characterization and Thermal Properties. *Materials* **2014**, *7*, 6105–6119. [[CrossRef](#)]
35. Zhang, X.; Yan, Q.; Li, J.; Zhang, J.; Cai, Z. Effects of Physical and Chemical States of Iron-Based Catalysts on Formation of Carbon-Encapsulated Iron Nanoparticles from Kraft Lignin. *Materials* **2018**, *11*, 139. [[CrossRef](#)] [[PubMed](#)]
36. Ju, X.; Bowden, M.; Brown, E.E.; Zhang, X. An improved X-ray diffraction method for cellulose crystallinity measurement. *Carbohydr. Polym.* **2015**, *123*, 476–481. [[CrossRef](#)] [[PubMed](#)]

37. Wunna, K.; Nakasaki, K.; Auresenia, J.L.; Abella, L.C.; Gaspillo, P.A.D. Effect of alkali pretreatment on removal of lignin from sugarcane bagasse. *Chem. Eng. Trans.* **2017**, *56*, 1831–1836. [[CrossRef](#)]
38. Popescu, C.-M.; Singurel, G.; Popescu, M.-C.; Vasile, C.; Argyropoulos, D.S.; Willför, S. Vibrational spectroscopy and X-ray diffraction methods to establish the differences between hardwood and softwood. *Carbohydr. Polym.* **2009**, *77*, 851–857. [[CrossRef](#)]
39. Kumar, P.; Barrett, D.M.; Delwiche, M.J.; Stroeve, P. Methods for Pretreatment of Lignocellulosic Biomass for Efficient Hydrolysis and Biofuel Production. *Ind. Eng. Chem. Res.* **2009**, *48*, 3713–3729. [[CrossRef](#)]
40. Dagnino, E.; Chamorro, E.; Romano, S.; Felissia, F.; Area, M. Optimization of the acid pretreatment of rice hulls to obtain fermentable sugars for bioethanol production. *Ind. Crop. Prod.* **2013**, *42*, 363–368. [[CrossRef](#)]
41. Renaudin, G.; Russias, J.; Leroux, F.; Frizon, F.; Cau-Dit-Coumes, C. Structural characterization of C–S–H and C–A–S–H samples—Part I: Long-range order investigated by Rietveld analyses. *J. Solid State Chem.* **2009**, *182*, 3312–3319. [[CrossRef](#)]
42. Renaudin, G.; Russias, J.; Leroux, F.; Cau-Dit-Coumes, C.; Frizon, F. Structural characterization of C–S–H and C–A–S–H samples—Part II: Local environment investigated by spectroscopic analyses. *J. Solid State Chem.* **2009**, *182*, 3320–3329. [[CrossRef](#)]
43. Yahia, A. Effect of solid concentration and shear rate on shear-thickening response of high-performance cement suspensions. *Constr. Build. Mater.* **2014**, *53*, 517–521. [[CrossRef](#)]
44. Roberti, F.; Cesari, V.F.; De Matos, P.R.; Pelisser, F.; Pilar, R. High- and ultra-high-performance concrete produced with sulfate-resisting cement and steel microfiber: Autogenous shrinkage, fresh-state, mechanical properties and microstructure characterization. *Constr. Build. Mater.* **2021**, *268*, 121092. [[CrossRef](#)]
45. Feys, D.; Verhoeven, R.; De Schutter, G. Why is fresh self-compacting concrete shear thickening? *Cem. Concr. Res.* **2009**, *39*, 510–523. [[CrossRef](#)]
46. Feys, D.; Verhoeven, R.; De Schutter, G. Fresh self compacting concrete, a shear thickening material. *Cem. Concr. Res.* **2008**, *38*, 920–929. [[CrossRef](#)]
47. Bender, J.W.; Wagner, N.J. Reversible shear thickening in monodisperse and bidisperse colloidal dispersions. *J. Rheol.* **1996**, *40*, 899–916. [[CrossRef](#)]
48. Mechtcherine, V.; Secieru, E.; Schröfl, C. Effect of superabsorbent polymers (SAPs) on rheological properties of fresh cement-based mortars—Development of yield stress and plastic viscosity over time. *Cem. Concr. Res.* **2015**, *67*, 52–65. [[CrossRef](#)]
49. Gwon, S.; Shin, M. Rheological properties of cement pastes with cellulose microfibers. *J. Mater. Res. Technol.* **2021**, *10*, 808–818. [[CrossRef](#)]
50. Aitcin, P.; Flatt, R.J. *Science and Technology of Concrete Admixtures*; Woodhead Publishing Limited: Sawston, UK, 2016; ISBN 9780081006931.
51. Montes, F.; Fu, T.; Youngblood, J.P.; Weiss, J. Rheological impact of using cellulose nanocrystals (CNC) in cement pastes. *Constr. Build. Mater.* **2020**, *235*, 117–132. [[CrossRef](#)]
52. Liu, J.; Khayat, K.H.; Shi, C. Effect of superabsorbent polymer characteristics on rheology of ultra-high performance concrete. *Cem. Concr. Compos.* **2020**, *112*, 103–126. [[CrossRef](#)]
53. Cyr, M.; Legrand, C.; Mouret, M. Study of the shear thickening effect of superplasticizers on the rheological behaviour of cement pastes containing or not mineral additives. *Cem. Concr. Res.* **2000**, *30*, 1477–1483. [[CrossRef](#)]
54. De Matos, P.R.; Jiao, D.; Roberti, F.; Pelisser, F.; Gleize, P.J. Rheological and hydration behaviour of cement pastes containing porcelain polishing residue and different water-reducing admixtures. *Constr. Build. Mater.* **2020**, *262*, 120–142. [[CrossRef](#)]
55. De Matos, P.R.; Sakata, R.D.; Gleize, P.J.P.; de Brito, J.; Repette, W.L. Eco-friendly ultra-high performance cement pastes produced with quarry wastes as alternative fillers. *J. Clean. Prod.* **2020**, *269*, 122–139. [[CrossRef](#)]
56. De Lima, A.C.P.; Bastos, D.L.R.; Camarena, M.A.; Bon, E.P.S.; Cammarota, M.C.; Teixeira, R.S.S.; Gutarra, M.L.E. Physicochemical characterization of residual biomass (seed and fiber) from açai (*Euterpe oleracea*) processing and assessment of the potential for energy production and bioproducts. *Biomass Convers. Biorefinery* **2019**, 1–11. [[CrossRef](#)]
57. Kochova, K.; Schollbach, K.; Gauvin, F.; Brouwers, H. Effect of saccharides on the hydration of ordinary Portland cement. *Constr. Build. Mater.* **2017**, *150*, 268–275. [[CrossRef](#)]
58. De Matos, P.R.; Sakata, R.D.; Onghero, L.; Uliano, V.G.; De Brito, J.; Campos, C.E.; Gleize, P.J. Utilization of ceramic tile demolition waste as supplementary cementitious material: An early-age investigation. *J. Build. Eng.* **2021**, *38*, 102–137. [[CrossRef](#)]
59. De Matos, P.R., Jr.; Pilar, R.; Gleize, P.J.P.; Pelisser, F. Use of recycled water from mixer truck wash in concrete: Effect on the hydration, fresh and hardened properties. *Constr. Build. Mater.* **2020**, *230*, 116–132. [[CrossRef](#)]
60. Gwon, S.; Choi, Y.C.; Shin, M. Effect of plant cellulose microfibers on hydration of cement composites. *Constr. Build. Mater.* **2021**, *267*, 121–142. [[CrossRef](#)]
61. Delannoy, G.; Marceau, S.; Glé, P.; Gourlay, E.; Guéguen-Minerbe, M.; Diafi, D.; Amziane, S.; Farcas, F. Impact of hemp shiv extractives on hydration of Portland cement. *Constr. Build. Mater.* **2020**, *244*, 118–137. [[CrossRef](#)]
62. Dils, J.; Boel, V.; De Schutter, G. Influence of cement type and mixing pressure on air content, rheology and mechanical properties of UHPC. *Constr. Build. Mater.* **2013**, *41*, 455–463. [[CrossRef](#)]
63. Kwasny, J.; Sonebi, M.; Plasse, J.; Amziane, S. Influence of rheology on the quality of surface finish of cement-based mortars. *Constr. Build. Mater.* **2015**, *89*, 102–109. [[CrossRef](#)]